Geophysical Journal International

Geophys. J. Int. (2017) **209,** 597–605
Advance Access publication 2017 January 25
GJI Seismology

doi: 10.1093/gji/ggx030

Simple estimation of linear 1+1 D long wave run-up

Mauricio Fuentes

Department of Geophysics, Faculty of Physical and Mathematical Sciences, University of Chile, Santiago, Chile. E-mail: mauricio@dgf.uchile.cl

Accepted 2017 January 23. Received 2017 January 20; in original form 2016 January 7

SUMMARY

An analytical solution is derived concerning the linear run-up for any given initial wave generated over a sloping bathymetry. Due to the simplicity of the linear formulation, complex transformations are unnecessary, hence the shoreline motion is directly obtained in terms of the initial wave. This result supports not only maximum run-up invariance between linear and nonlinear theories but also the time evolution of shoreline motion and velocity, exhibiting good agreement with the nonlinear theory. The present formulation also allows quantifying the shoreline motion numerically from a customized initial waveform, including non-smooth functions. This is useful for numerical tests, laboratory experiments or realistic cases in which the initial disturbance might be retrieved from seismic data rather than using a theoretical model. It is also shown that the run-up calculation for the real case studied is consistent with the field observations.

Key words: Numerical approximations and analysis; Tsunamis; South America.

1 INTRODUCTION

In near field subduction zones, after an earthquake triggers a tsunami, the first wave reaches the coastline within 15–30 min. Nevertheless, in the recent 2015 Illapel tsunami, witnesses affirm that the first inundation occurred 5 min after origin time (Melgar *et al.* 2016). The short response-time motivates an analytical study to understand the local phenomena in coastal zones.

The 1+1 D (one space + one temporal dimension) water wave evolution problem over sloping bathymetries has been extensively studied. Contributions regarding the run-up problem on sloping beaches have been addressed for over five decades. The first solution for the fully nonlinear formulation of the shallow water wave equations on a sloping beach (Fig. 1a) was presented by Carrier & Greenspan (1958). They defined a hodograph transformation (the CG transformation) in terms of the Riemann invariants of the hyperbolic system that connects the physical space (x, t) with a dual space (σ, λ). Tuck & Hwang (1972) proposed a slightly different transformation that not only solves the nonlinear equations but also turns them into the same form as the linear ones.

Another approach is having a sloping beach consisting of a uniform sloping part connected to a horizontal plane that models the average sea floor (the canonical problem (Fig. 1b)). Synolakis (1987) considered an incoming solitary wave into the canonical problem. The author derived an analytical expression for the run-up, referred to as run-up law hereafter. He also studied the nonlinear effects with the use of the CG transformation, providing a wave breaking criterion. His work is widely used as a benchmark for numerical codes (Synolakis *et al.* 2008), and it has been the base to further approaches. Li & Raichlen (2001) confirmed the wave breaking criterion obtained by Synolakis (1987), with numerical and experimental approaches. Besides, Li & Raichlen (2001) added a correction term to the run-up law derived by Synolakis (1987), which is important in a specific range of relative wave height, but neglects most of the geophysical applications. Pelinovsky & Mazova (1992) considered different initial waveforms to investigate the analytical solution of the nonlinear run-up problem. They included a parameter in order to describe the domain of a wave breaking region. They confirmed its importance and its application for real tsunamis by taking a database of over 114 events. They tested their results with monochromatic waves and Lorenz pulses.

Motivated by tsunami observations of the M_w 7.7 1992 Nicaraguan Earthquake, Tadepalli & Synolakis (1994) introduced N-shaped waves, namely N-waves. They are suitable for subduction zones where the subducting plate angle is more gradual, and the earthquake can produce an initial wave with a visible elevation-subsidence pattern.

Liu *et al.* (2003) solved the forced linear shallow water equation. They compared their solution with the nonlinear depth integrated version of the same problem in order to study the run-up process of landslides.

An analytic solution of the nonlinear shoreline motion and velocity on a sloping beach was presented by Kânoğlu (2004). He utilized the linearized CG transformation, and succeeded in describing the run-up process for several waves: Gaussian pulse, solitary wave and N-wave. In the same line, Pritchard & Dickinson (2007) extended the Kânoğlu's (2004) solution using a near-shore expansion around of the transformed shoreline coordinate, which is valid for any smooth initial condition. Those initial waves are approximated by a combination of Gaussian waveforms proposed by Carrier *et al.* (2003).

© The Author 2017. Published by Oxford University Press on behalf of The Royal Astronomical Society.

Downloaded from https://academic.oup.com/gji/article-abstract/209/2/597/2957020
by Universidad de Chile user
on 22 March 2018

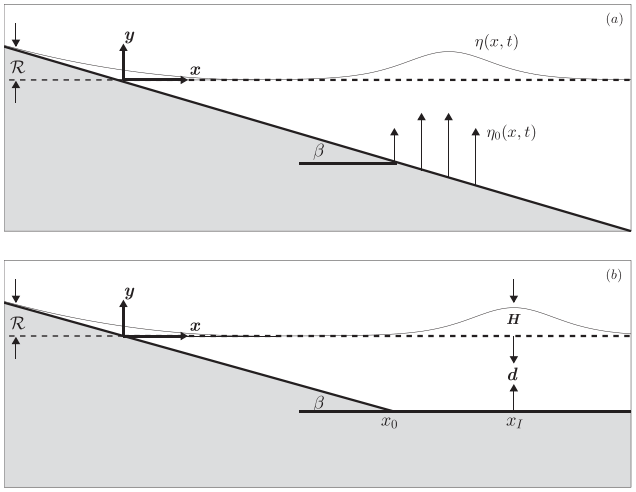

Figure 1. Sketches of the basic models including the variable definitions and coordinate system. (a) Sloping uniform beach geometry. (b) Canonical problem geometry.

Madsen *et al.* (2008) made a complete review in relation to the use of solitary waves for tsunami modelling. They stated that there are not enough arguments to utilize solitary-type wave as an initial condition, at least in geophysical scales and, as Kânoğlu *et al.* (2015) pointed out, this paradigm shifts from solitary to N-wave. Additionally, Madsen & Schäffer (2010) provided an analytical solution for the full nonlinear shallow water equations by using the CG transformation. They applied their solution to well-known initial waves, for instance, sinusoidal, solitary, and N-waves. However, as Madsen & Schäffer (2010) pointed-out, the solution is applicable only for smooth enough initial conditions.

Other approaches have been studied regarding complex features. Kânoğlu & Synolakis (1998) and Fuentes *et al.* (2015) studied the linear 1+1 D run-up for an extended case of the canonical problem. Instead of using the canonical setting, they considered a piecewise linear bathymetry, by finding a strong dependence of the run-up with the slope of the closest segment to the shore. Ezersky *et al.* (2013) and Fuentes *et al.* (2015) used this approach to explore resonance effects attributed to bathymetry shape. Fuentes *et al.* (2013) incorporated dimensional complexity regarding the 2+1 D problem (x, y, t). They provided an analytical solution for a solitary wave in an extended canonical problem. Recently, Riquelme *et al.* (2015) used these two approaches and proposed a quick way to estimate the run-up heights as soon as the seismic information allows imaging of the earthquake source. Kânoğlu *et al.* (2013) provide a 2+1 D approach on a constant depth ocean inside the linear regime. Their solution reveals important focusing phenomena of N-waves, that is to say, the convergence of waves on a certain focal point. Sepúlveda & Liu (2016) proposed an analytic solution based on a Fourier expansion of the initial condition in terms of the fault plane parameters.

This work presents a simple analytical solution for the linear run-up height on a sloping beach, allowing even the use of non-smooth initial waves. This solution can be used to integrate any kind of wave, in particular, those obtained from seismic data. The mathematical development is presented in Section 2. A complete and detailed derivation of the whole development is shown in the appendix. In Section 3, a comparison between the present solution with the full nonlinear solution is given. Different kind of classic waves are tested, including a real tsunami case. Finally, a summary and main conclusions are given in Section 4.

2 MATHEMATICAL DERIVATION

A tsunami run-up is generally modelled with shallow water equations. This study focuses on the 1+1 D linear formulation. Since it was pointed out by Synolakis (1991), the linear theory can correctly predict the run-up on a sloping beach for a non-breaking initial wave. Thus, the linear equations to consider are

$$u_t + \mathrm{g}\eta_x = 0 \tag{1}$$

$$\eta_t + [hu]_x = \eta_{0t} \tag{2}$$

where $u = u(x, t)$ represents the depth-averaged horizontal velocity component, $\eta(x, t)$ is the water surface disturbance, $\eta_0(x, t)$ is a forcing term, which models the sea floor deformation, $h = h(x)$ is the bathymetry profile and g the gravity acceleration. Hereafter, the slope of the beach will be referred to as $\alpha =: \tan(\beta)$. In the present case, $h(x) = \alpha x$, which means that the problem to solve is set in Fig. 1(a).

Tuck & Hwang (1972) utilized the system (1)–(2), and derived an expression for η by the standard Hankel–Laplace transform technique, obtaining:

$$\eta(x,t) = \frac{2}{\sqrt{\mathrm{g}\alpha}} \int_0^\infty J_0\left(2k\sqrt{x}\right) \int_0^\infty J_0\left(2k\sqrt{\xi}\right) \times \int_0^t \eta_{1tt}(\xi,\tau)\sin[\sqrt{\alpha}\mathrm{g}k(t-\tau)]\mathrm{d}\tau\,\mathrm{d}\xi\,\mathrm{d}k, \tag{3}$$

where

$$\eta_1(x,t) = \eta_0(x,t) + [\eta(x,0_-) + t\eta_t(x,0_-)]\mathcal{H}(t), \tag{4}$$

$\mathcal{H}(t)$ is the Heaviside step function and $J_0(\cdot)$ is the zero-order cylindrical Bessel function. Note that the notation '0_-' in eq. (4) comes from the Laplace transform that allows the use of generalized functions (see Appendix A1).

When it is desired to account for the effects of the tsunami generation process, it is important to consider a time-dependent forcing term $\eta_0(x, t)$ which contains the time history of a seismic source. This could be particularly useful for slow earthquake or landslide (Liu *et al.* 2003) generated tsunamis. In these cases $\eta(x, 0_-) = \eta_t(x, 0_-) = 0$. However, because generally tsunami speed is approximately 15 times slower than rupture velocity, a common practice is to consider an instantaneous initial wave transferred from the seabed to the water surface, keeping the same shape. This is equivalent to the absence of the term $\eta_0(x, t)$. Also, Synolakis *et al.* (1997) pointed out that for an initial value tsunami problem, a null initial velocity should be taken ($u(x, 0) = \eta_t(x, 0_-) = 0$). However, there are solutions accounting for an initial velocity different from zero (Kânoğlu & Synolakis 2006). Thus, from (4)

$$\eta_{1tt}(x,t) = \eta(x,0_-)\delta_t(t) \tag{5}$$

and expression (3) yields

$$\eta(x,t) = \frac{2}{\sqrt{\mathrm{g}\alpha}} \int_0^\infty \eta(\xi,0_-)G_t(x,\xi,t)\mathrm{d}\xi \tag{6}$$

where

$$G(x,\xi,t) = \int_0^\infty J_0\left(2k\sqrt{x}\right) J_0\left(2k\sqrt{\xi}\right)\sin[\sqrt{\alpha}\mathrm{g}tk]\mathrm{d}k \tag{7}$$

which was obtained by Tuck & Hwang (1972). Eqs (6) and (7) are the starting point of this paper. Carrier *et al.* (2003) practically obtained the same kernel as eq. (7), interpreted as a Green function in the hodograph space for the nonlinear solution. They derived an

Downloaded from https://academic.oup.com/gji/article-abstract/209/2/597/2957020
by Universidad de Chile user
on 22 March 2018

explicit formula in terms of the complete elliptic integral of first kind.

Also, from eqs (6) and (7), one can derive the shoreline velocity in terms of the initial wave (see Appendix A2 for details),

$$u(0,t) = -\frac{1}{\alpha}\eta_t(0,t). \tag{8}$$

Accounting for the moving boundary condition at the shoreline is a difficult task to solving. Normally, the run-up is attained for a coordinate inland ($x < 0$, and nonlinear theory must be used), however, to study the approximate shoreline motion with linear theory, the still-water shoreline is considered (hereafter SWS), that is to say, the water height at the shoreline of the undisturbed water level. Thus, evaluating at $x = 0$, eq. (7) reduces to

$$G(0,\xi,t) = \frac{1}{2}\frac{\mathcal{H}\left(\frac{1}{4}\alpha g t^2 - \xi\right)}{\sqrt{\frac{1}{4}\alpha g t^2 - \xi}} \tag{9}$$

therefore, from eqs (6) and (9), the time-series at the shoreline is

$$\eta(0,t) = \frac{1}{2}\frac{\partial}{\partial t}\left\{ t\int_0^1 \frac{\eta\left(\frac{1}{4}\alpha g t^2 y, 0_-\right)}{\sqrt{1-y}}\mathrm{d}y \right\}. \tag{10}$$

Note that eq. (10) does not require derivatives of the initial condition, which allows the use of less restrictive waves than the standard formulations. This is the main result of this work. Eq. (10) gives the SWS in terms of the initial condition only, in a quite simple integral representation. When the initial condition is set, the use of this formula allows for prompt estimation of the SWS and the corresponding maximum run-up.

Numerical integration can be used to evaluate eq. (10). However, if the initial condition corresponds to an infinitely differentiable function, by doing integration by parts N times, the integral on eq. (10) is equivalent to

$$\int_0^1 \frac{\eta(x^* y, 0_-)}{\sqrt{1-y}}\mathrm{d}y = 2\sum_{k=0}^{N-1}\frac{(2x^*)^k}{(2k+1)!!}\partial_x^k\eta(0,0_-) + \frac{(2x^*)^N}{(2N-1)!!}\int_0^1 (1-y)^{N-\frac{1}{2}}\partial_x^N\eta(x^* y, 0_-)\mathrm{d}y \tag{11}$$

where $x^* = \frac{1}{4}\alpha g t^2$.

The remainder in eq. (11) tends to zero when N tends to infinity. Thus, an explicit power series is obtained for the approximated shoreline motion:

$$\eta(0,t) = \sum_{k=0}^{\infty}\frac{(2x^*)^k}{(2k-1)!!}\partial_x^k\eta(0,0_-) \tag{12}$$

which is suitable when McLaurin coefficients can be computed explicitly. An equivalent and more elegant manner for deriving expression (12) is to apply eq. (10) by expanding $\eta(x, 0_-)$ in the McLaurin series and using the Beta function:

$$\int_0^1 \frac{y^k}{\sqrt{1-y}}\mathrm{d}y = \mathrm{B}\left(k+1,\frac{1}{2}\right) = \frac{2^{k+1}k!}{(2k+1)!!}.$$

According to the linear theory, the maximum run-up and run-down can be obtained by solving the following optimization problems

$$\mathcal{R}_{\mathrm{up}} = \max_{t\in\mathrm{R}_+}\eta(0,t) \tag{13}$$

$$\mathcal{R}_{\mathrm{down}} = \min_{t\in\mathrm{R}_+}\eta(0,t). \tag{14}$$

For $x < 0$, the previous formulation is not valid and one must solve the nonlinear equations (Synolakis 1987, 1991).

3 INITIAL WAVES TESTED

Formulae (10) and (12) allow the evaluation for any type of initial wave. Customized shapes can also be evaluated, even if they do not proceed from usual functions. Even though the whole development was made in dimensional form, it can be easily converted into the dimensionless form by replacing $\alpha = \mathrm{g} = 1$.

3.1 Analytical solution: parabolic wave

For analytical purposes, knowing precise expressions is useful for validating new solutions and numerical codes. In this case, the initial wave of maximum height H at $\frac{x_0}{2}$ is defined as

$$\eta(x,0_-) = 4H\left(1-\frac{x}{x_0}\right)\frac{x}{x_0}\mathcal{H}(x_0-x). \tag{15}$$

This wave is not smooth at $x = x_0$, however, it is still possible to use it as initial condition. A direct evaluation from eq. (12) shows the maximum run-up is $\mathcal{R}_{\mathrm{up}} = \frac{3}{2}H$, occurs at the time $t_{\mathrm{up}} = \sqrt{\frac{3x_0}{2\alpha g}}$, and the run-down $\mathcal{R}_{\mathrm{down}} = -\frac{8}{3}H$ is reached at the time $t_{\mathrm{down}} = \sqrt{\frac{4x_0}{\alpha g}}$.

Fig. 2 shows the computed SWS motion for different initial parabolic waves. The numerical integration of eq. (10) confirms the analytical solution for the run-up and the run-down.

3.2 Gaussian pulse

A good way to validate analytical solutions is to compare them with the existing ones. In this case, those solutions presented by Carrier *et al.* (2003) are considered. By using the nonlinear theory, they computed the maximum run-up and run-down for four different initial waves constructed with Gaussian pulses of the form

$$\eta(x,0_-) = H_1\exp\left\{-k_1(x-x_1)^2\right\} - H_2\exp\left\{-k_2(x-x_2)^2\right\} \tag{16}$$

Fig. 3 shows the initial waves and the SWS motions. The analytical solutions obtained in eqs (10) and (8) exhibit good agreement in comparison with results obtained by Carrier *et al.* (2003).

3.3 Solitary wave

The most regular solution of the Korteweg–De Vries equation is known as a solitary wave, and it takes the form

$$\eta(x,0_-) = H\mathrm{sech}^2(\gamma(x-x_1)) \tag{17}$$

with $\gamma = \frac{1}{d}\sqrt{\frac{3H}{4d}}$.

Synolakis (1987) obtained the maximum run-up of this wave in the canonical problem, namely $\mathcal{R}_{\mathrm{up}} = 2.831H^{\frac{5}{4}}d^{-\frac{1}{4}}|\alpha|^{-\frac{1}{2}}$.

Fig. 4 shows the results of four different solitary waves studied by Kânoğlu (2004) used to validate his own analytical solution. The presented solution accurately predicts the run-up values. The dependence of the maximum run-up with the initial height is confirmed inside the linear regime, as Synolakis (1987) pointed out.

3.4 N-waves

Tadepalli & Synolakis (1994) defined a dipole wave in terms of hyperbolic functions. They followed the same formalism proposed by Synolakis (1987) to describe the run-up process of the solitary

Downloaded from https://academic.oup.com/gji/article-abstract/209/2/597/2957020
by Universidad de Chile user
on 22 March 2018

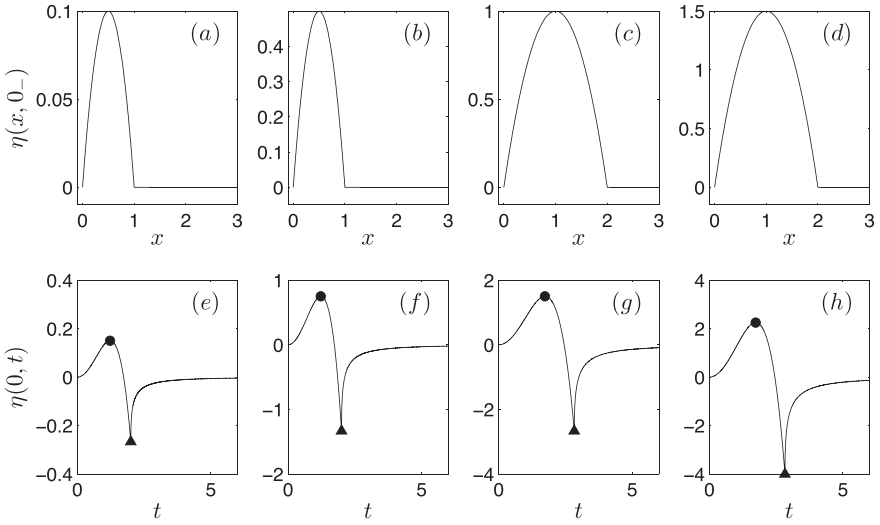

Figure 2. Four parabolic initial waves (a)–(d) from eq. (15) and their corresponding SWS motion (e)–(h) evaluated from eq. (10) in dimensionless form. Circles and triangles are the analytical run-up and run-down, respectively. (a) $H = 0.1$ and $x_0 = 1$. (b) $H = 0.5$ and $x_0 = 1$. (c) $H = 1$ and $x_0 = 2$. (d) $H = 0.1$ and $x_0 = 2$.

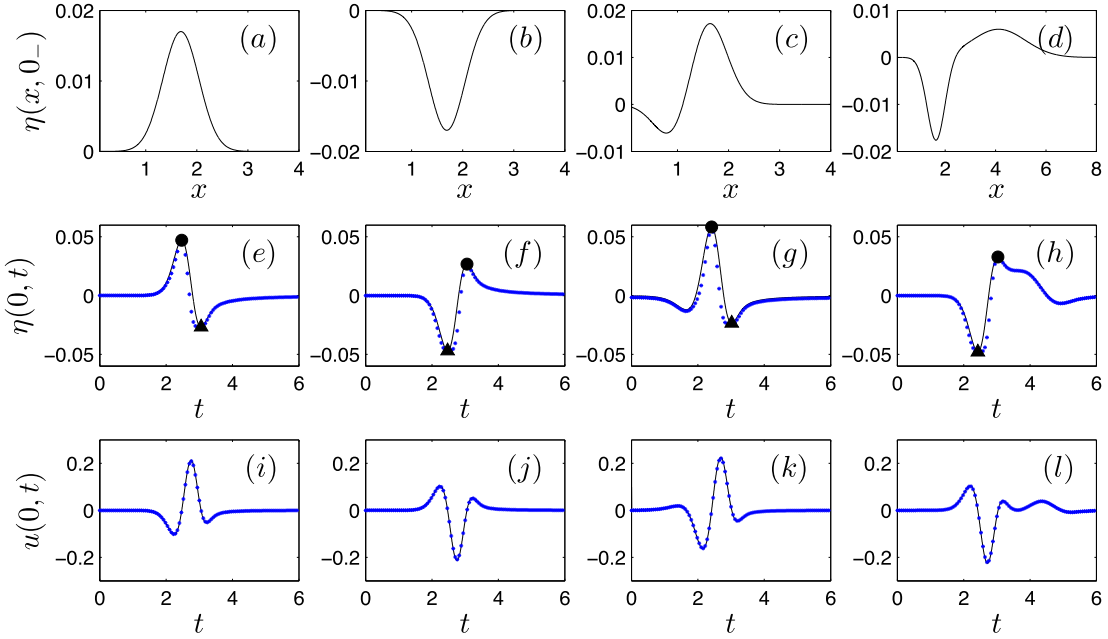

Figure 3. Four Gaussian initial waves (a)–(d) from eq. (18) and their corresponding SWS motion (e)–(h) evaluated from eq. (10) and shoreline velocities (i)–(l) from eq. (8) in dimensionless form. In (e)–(l), the continuous line represents the linear theory (eqs 10 and 8) and the blue dots, the nonlinear theory (Kânoğlu 2004). (a) $H_1 = 0.017$, $x_1 = 1.69$, $k_1 = 4$, $H_2 = x_2 = k_2 = 0$. (b) $H_1 = -0.017$, $x_1 = 1.69$, $k_1 = 4$, $H_2 = x_2 = k_2 = 0$. (c) $H_1 = 0.02$, $x_1 = 1.5625$, $k_1 = 3.5$, $H_2 = 0.01$, $x_2 = 1$, $k_2 = 3.5$. (d) $H_1 = 0.006$, $x_1 = 4.1209$, $k_1 = 0.4444$, $H_2 = 0.018$, $x_2 = 1.6384$, $k_2 = 4$. The pairs $\mathcal{R}_{\rm up} - \mathcal{R}_{\rm down}$ are (e) 0.0471 and −0.0268. (f) 0.0268 and −0.0471. (g) 0.0584 and −0.0235. (h) 0.0328 and −0.0481.

wave in the canonical problem. The expression for an isosceles leading-elevation, or depression N-wave, is

$$\eta(x, 0_-) = \pm \frac{3\sqrt{3}}{2} H \mathrm{sech}^2(\gamma(x - x_1)) \tanh(\gamma(x - x_1)) \qquad (18)$$

with $\gamma = \frac{3}{2d}\sqrt{\frac{3}{4}\frac{H}{d}}$. They obtained that $\mathcal{R}_{\rm up} = 3.86 H^{\frac{5}{4}} d^{-\frac{1}{4}} |\alpha|^{-\frac{1}{2}}$.

Fig. 5 shows the results for four different isosceles N-waves studied by Kânoğlu (2004). The reader may note the symmetry between the run-up and run-down with leading-elevation and depression N-wave. As it was shown by Tadepalli & Synolakis (1994), for a leading-elevation isosceles N-wave in a canonical problem, $\mathcal{R}_{\rm up}$, $\mathcal{R}_{\rm down} \propto H^{\frac{5}{4}}$, which is in agreement with the results obtained.

3.5 A case study: the 2014 $M_{\rm w} = 8.2$ Iquique earthquake

As it has been said before, the computation for the SWS motion can be performed for any initial wave, including a discrete description of the profile. However, numerical integration requires a special care for this case. First, the singularity on the integrand in eq. (10) is removed by a simple trigonometric change of variables, namely $y = \sin^2(\theta)$. Then, the integral $I(t)$ is approximated with a

Downloaded from https://academic.oup.com/gji/article-abstract/209/2/597/2957020
by Universidad de Chile user
on 22 March 2018

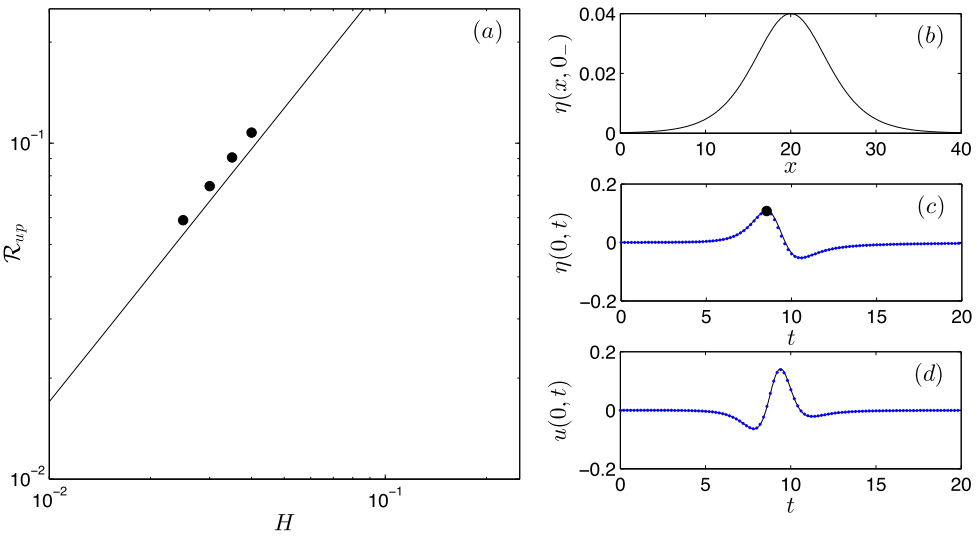

Figure 4. Results for four solitary waves in dimensionless form. (a) Black dots represent the run-up computed from eq. (10), $H = 0.040, 0.035, 0.030, 0.025$ and $x_1 = 20$. The line shows $\mathcal{R}_{up} \propto H^{\frac{5}{4}}$. (b) Example of initial solitary wave with $H = 0.040$ and $x_1 = 20$. (c,d) represent the SWS motion and shoreline velocity respectively for the initial wave shown in (b). Black continuous lines show the linear solutions (eq. 10 for (c) and eq. 8 for (d)) and the blue dots are the nonlinear solutions from Kânoğlu (2004).

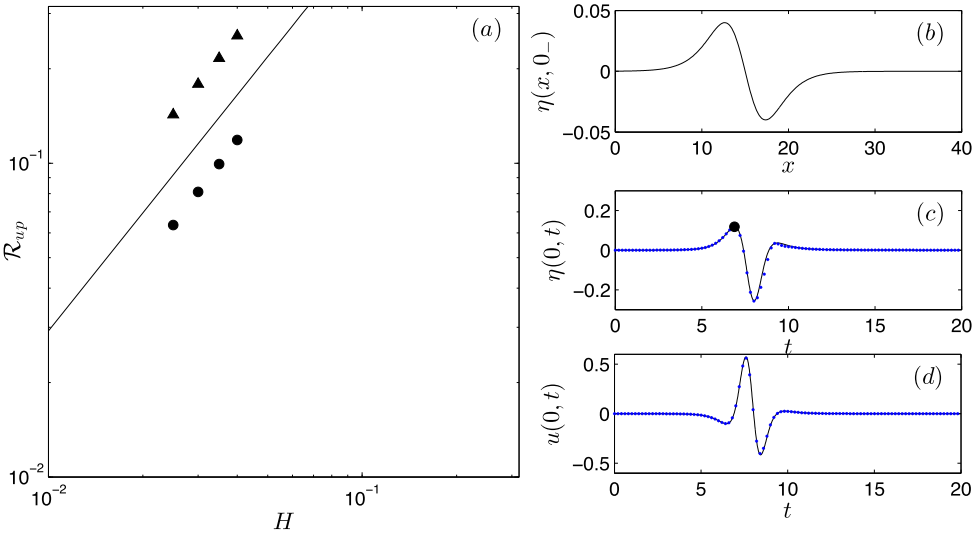

Figure 5. Results for four Isosceles N-waves in dimensionless form. (a) Black dots represent the run-up and black triangles, the run-down computed from eq. (10), with $H = 0.040, 0.035, 0.030, 0.025$ and $x_1 = 15$. The line shows that $\mathcal{R}_{\text{up}}, \mathcal{R}_{\text{down}} \propto H^{\frac{5}{4}}$. (b) Example of initial leading elevation Isosceles N-wave with $H = 0.040$ and $x_1 = 15$. (c) and (d) represent the SWS motion and shoreline velocity respectively for the initial wave shown in (b). Black continuous lines show the linear solutions (eq. 10 for (c) and eq. 8 for (d)) and the blue dots are the nonlinear solutions from Kânoğlu (2004).

trapezoidal method of non-uniform grid,

$$I(t) =: \int_0^1 \frac{\eta\left(\frac{1}{4}\alpha g t^2 y, 0_-\right)}{\sqrt{1-y}}\mathrm{d}y$$
$$= 2\int_0^{\frac{\pi}{2}} \eta\left(\frac{1}{4}\alpha g t^2 \sin^2(\theta), 0_-\right)\sin(\theta)\mathrm{d}\theta. \tag{19}$$

The observations for the initial wave are defined as (x_i, η_i). The discretization is given by $x_m = \frac{m-1}{N_x-1}X_f,\ m = 1, \ldots N_x$, with X_f the length of the profile. The discretization of the time variable is $t_j = \frac{j-1}{N_t-1}T_f,\ j = 1, \ldots, N_t$, with T_f the time duration of the simulation. The discretization of the interval $[0, \frac{\pi}{2}]$ is given by $\theta_i = \arcsin(\sqrt{\frac{i-1}{N_0-1}}),\ i = 1, \ldots, N_0$. For obtaining a correct evaluation of the integral, there should be a matching along the discretization. This implies $X_f = \frac{1}{4}\alpha g T_f^2$ and $N_x = 1 + (N_0 - 1)(N_t - 1)^2$.

The numerical approximation of the integral $I(t)$, for large values of N_0 is

$$I_j =: I(t_j) \approx \sum_{i=1}^{N_0-1}\left(\eta_{m(i+1,j)}\sqrt{\frac{i}{N_0-1}} + \eta_{m(i,j)}\sqrt{\frac{i-1}{N_0-1}}\right)$$
$$\times(\theta_{i+1} - \theta_i) + \mathcal{O}\left(N_0^{-\frac{1}{2}}\right) \tag{20}$$

with $m(i, j) = 1 + (i - 1)(j - 1)^2$. The order of approximation comes from the truncation error of trapezoidal rule of non-uniform grid spacing.

Finally, the approximated shoreline motion for the observed initial wave is

$$\eta(0, t_j) \approx \frac{1}{2}\left\{jI_{j+1} - (j-1)I_j\right\} \quad j = 1, \ldots, N_t - 1. \tag{21}$$

Downloaded from https://academic.oup.com/gji/article-abstract/209/2/597/2957020
by Universidad de Chile user
on 22 March 2018

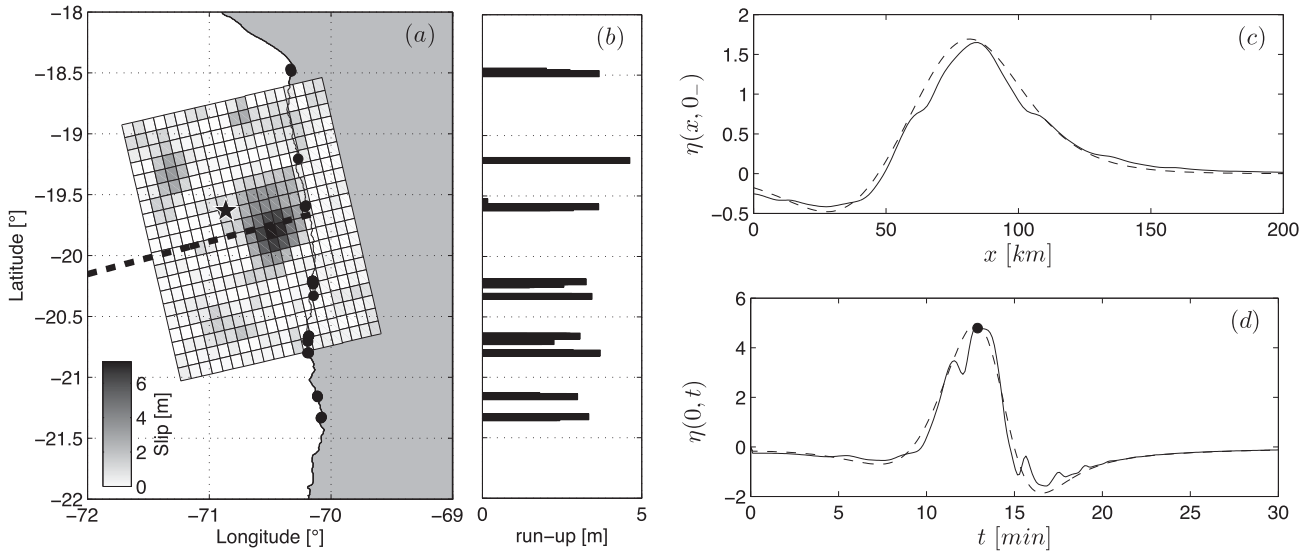

Figure 6. Comparison between two initial waves: one from teleseismic data and the other from a theoretical N-wave. (a) Finite Fault Model of the $M_w = 8.2$ Iquique Earthquake (Hayes *et al.* 2014). The black star represents the epicentre, and dots are the field measurements locations and the dashed line represents the chosen transect. (b) Field measurements of the run-up heights of the 2014 Iquique tsunami. (c) Initial profile along the transect shown in (a). The continuous curve represents the initial wave obtained from the slip model in (a). The dashed line represents a generalized N-wave (Madsen & Schäffer 2010) with $A_1 = 1.7\,\text{m}$, $A_2 = 0.7\,\text{m}$, $x_1 = 82\,\text{km}$, $x_2 = 35.8\,\text{km}$ and $\gamma = 0.0340\,\text{km}^{-1}$ (eq. 22). (d) SWS motions for the initial waves shown in (c). The time-series derived from seismic data (continuous) is computed with eqs (20)–(21), while theoretical N-wave (dashed) is computed with eq. (10). Black dot represents the maximum run-up of the analytical solution.

After an earthquake occurs, teleseismic inversion is performed in order to reconstruct the distribution of the slip across the fault plane, and then, a Finite Fault Model (FFM) is generated. The FFM used for the $M_w = 8.2$ Iquique earthquake is obtained from the USGS website (Hayes *et al.* 2014). Once the FFM is available, it is possible to derive the initial condition from Okada's equations (Okada 1985), which provides the static sea floor deformation. In the formulation presented in this paper, the static deformation is directly transferred to the water surface as an initial condition. Fig. 6 shows the FFM model and the initial waveform produced along the maximum uplift zone in order to obtain $\eta(x, 0_-)$.

The maximum run-up is a combination of the first wave impact and excitation of the resonance modes. Later edge waves can amplify the run-up, as it was observed in the Iquique earthquake (An *et al.* 2014; Catalán *et al.* 2015). However, to anticipate the tsunami hazard, it is worth to estimate the first impact. Riquelme *et al.* (2015) utilized analytical solutions from Fuentes *et al.* (2013, 2015) to propose a methodology to obtain an approximated run-up distribution as soon as the seismic information is retrieved (Fig. 6), obtaining estimations of the same order as the ones observed by field measurements.

In order to compare the numerical integration with the analytical solution, a generalized N-wave is chosen (Madsen & Schäffer 2010). The initial wave is defined as

$$\eta(x, 0_-) = A_1 \text{sech}^2(\gamma(x - x_1)) - A_2 \text{sech}^2(\gamma(x - x_2)), \tag{22}$$

where $\gamma(x_1 - x_2) = \frac{\pi}{2}$. The run-up in a canonical problem for these kinds of waves (presented in an equivalent form) is

$$\mathcal{R}_{\text{up}} = A_1 \sqrt{\gamma d} |\alpha|^{-\frac{1}{2}} \max_{\theta} \chi_\mu(\theta), \tag{23}$$

where $\mu = \frac{A_2}{A_1}$, $\chi_\mu(\theta) = \text{Li}(-\frac{3}{2}, -\text{e}^{-2\theta}) - \mu \text{Li}(-\frac{3}{2}, -\text{e}^{-2\theta+\pi})$, $\text{Li}(n, \lambda)$ is the polylogarithm function and θ is a time variable (Madsen & Schäffer 2010).

Table 1. Summary of relative error (per cent) of waves tested from Sections 3.2–3.4. $|\mathcal{R}_{\text{non linear}} - \mathcal{R}_{\text{linear}}|/\mathcal{R}_{\text{non linear}}$ is around 0–2 per cent.

	Gaussian	Solitary	N-wave
(a)	0.0298	0.0030	1.5603
(b)	0.1381	0.0056	1.3453
(c)	2.3613	0.0048	1.0744
(d)	0.1319	0.0288	0.7997

Fig. 6 shows that the analytical shoreline motion for the initial wave obtained from the FFM agrees with the modelled N-shaped wave, despite the fact that the curve obtained from seismic data does not come from an elementary function. By using typical values for northern Chile ($d = 4\,\text{km}$ and $\alpha = \frac{1}{20}$), the run-up of the generalized theoretical N-wave is 5.8 m according to eq. (23). The run-up is 4.7 m in the case of the disturbance produced with the Okada's equations, which are consistent with the observed field measurements of the order of 4 m (Catalán *et al.* 2015). It is interesting to note that the analytical solution provided by Sepúlveda & Liu (2016), with the seismic parameters found in Hayes *et al.* (2014), yields a run-up of 4.2 m, which is also consistent with the results of this work.

4 DISCUSSION AND CONCLUSIONS

An analytical solution is computed to model the shoreline motion derived from linear theory, and a method to integrate any type of initial waves is developed.

The complexity in the treatment of the nonlinear solutions consists in passing from the physical into the dual space, and vice versa. Also, most of available analytical solutions are restricted to smooth waves only. The derived solution from the linear theory overcomes this issue, producing a fast computation, with almost the same accuracy as the nonlinear theory, as shown in Table 1. However, the present solution is valid for profiles only, that is to say that some

Downloaded from https://academic.oup.com/gji/article-abstract/209/2/597/2957020
by Universidad de Chile user
on 22 March 2018

important 2-D effects can be missed, for instance, wave focusing (Kânoğlu *et al.* 2013) and interference are neglected.

This formulation can be adapted to integrate any kind of initial wave, even an arbitrary waveform that, for example, may be retrieved from seismic data. However, additional work should be done in order to explore the range of validity and sensitivity of the parameters.

As it was presented in the introduction, the state of the art already has analytical solutions, even for nonlinear theory. Also, the long wave run-up invariance between linear and nonlinear theories has been well documented. Nonetheless, the present solution also shows full shoreline motion and velocity invariance. One advantage of linear solutions in dimensional form is to allow direct physical and mathematical interpretation from the initial condition and the geometrical setting. On the other hand, this approach has some limitations regarding the scope of the solution. Due to some important 2+1 D effects ignored along the wave travel (e.g. wave focusing, energy loss, etc.), far field tsunamis are not suitable to consider here. It will be worth it to dedicate a future work to explore the generalization of this approach to higher dimensions.

For tsunami early warning purposes, a first order run-up estimation is necessary. Then, an analytical solution adapted for tsunami generation on a sloping bathymetry, rather than a plane sea floor, is more realistic. In terms of efficient estimation, Riquelme *et al.* (2015) proposed the idea to use analytical water wave solutions, utilizing FFMs, that could be rapidly generated by GPS inversions (≈5 min). An improvement to their methodology is to replace the 1+1 D formulation with the one presented here, which is more suitable for subduction zones, and that practically does not need computational time to be evaluated.

ACKNOWLEDGEMENTS

This work was entirely supported by the *Programa de Riesgo Sísmico*. The author thanks to an anonymous reviewer for his insightful comments, which helped to improve the manuscript.

REFERENCES

Abramowitz, M. & Stegun, I.A., 1964. *Handbook of Mathematical Functions: With Formulas, Graphs, and Mathematical Tables (No. 55),* Courier Corporation.

An, C., Sepúlveda, I. & Liu, P.L., 2014. Tsunami source and its validation of the 2014 Iquique, Chile Earthquake, *Geophys. Res. Lett.,* **41**(11), 3988–3994.

Carrier, G. & Greenspan H., 1958. Water waves of finite amplitude on a sloping beach, *J. Fluid Mech.,***4**(1), 97–109.

Carrier, G.O., Wu, T.T. & Yeh, H., 2003. Tsunami run-up and draw-down on a plane beach, *J. Fluid Mech.,* **475,** 79–99.

Catalán, P. *et al.*, 2015. The 1 April 2014 Pisagua tsunami: observations and modeling, *Geophys. Res. Lett.,* **42,** 2918–2925.

Ezersky, A., Tiguercha, D. & Pelinovsky, E., 2013. Resonance phenomena at the long wave run-up on the coast, *Nat. Hazards Earth Syst. Sci.,* **13**(11), 2745–2752.

Fuentes, M., Ruiz, J. & Cisternas, A., 2013. A theoretical model of tsunami runup in Chile based on a simple bathymetry, *Geophys. J. Int.,* **196**(2), 986–995.

Fuentes, M., Ruiz, J. & Riquelme, S., 2015. The runup on a multilinear sloping beach model, *Geophys. J. Int.,* **201**(2), 915–928.

Gradshteyn, I.S. & Ryzhik, I.M., 1994. *Table of Integrals, Series, and Products,* Academic.

Hayes, G. *et al.*, 2014. Continuing megathrust earthquake potential in Northern Chile after the 2014 Iquique earthquake sequence, *Nature,* **512**(7514), 295–298.

Kânoğlu, U., 2004. Nonlinear evolution and runup–rundown of long waves over a sloping beach, *J. Fluid Mech.,* **513,** 363–372.

Kânoğlu, U. & Synolakis C., 1998. Long wave runup on piecewise linear topographies, *J. Fluid Mech.,* **374,** 1–28.

Kânoğlu, U. & Synolakis, C., 2006. Initial value problem solution of nonlinear shallow water-wave equations, *Phys. Rev. Lett.,* **97**(14), 148501.

Kânoğlu, U., Titov, V.V., Aydin, B., Moore, C., Stefanakis, T.S., Zhou, H., Spillane, M. & Synolakis, C.E., 2013. Focusing of long waves with finite crest over constant depth, *Proc. R. Soc. A,* **469**, 2153, 20130015.

Kânoğlu, U., Titov, V., Bernard, E. & Synolakis, C., 2015. Tsunamis: bridging science, engineering and society, *Phil. Trans. R. Soc. A*, **373**, 2053, 20140369.

Li, Y. & Raichlen, F., 2001. Solitary wave runup on plane slopes, *J. Waterway Port Coast. Ocean Eng.,* **127**(1), 33–44.

Li, Y. & Raichlen, F., 2002. Non-breaking and breaking solitary wave run-up, *J. Fluid Mech.,* **456,** 295–318.

Liu, P.L.-F., Lynett, P. & Synolakis, C., 2003. Analytical solutions for forced long waves on a sloping beach, *J. Fluid Mech.,* **478,** 101–109.

Madsen, P.A. & Schäffer, H.A., 2010. Analytical solutions for tsunami runup on a plane beach: single waves, N-waves and transient waves, *J. Fluid Mech.,* **645,** 27–57.

Madsen, P.A., Fuhrman, D.R. & Schäffer, H.A., 2008. On the solitary wave paradigm for tsunamis, *J. geophys. Res.,* **113,** 1–22.

Melgar D. *et al.*, 2016. Slip segmentation and slow rupture to the trench during the 2015, Mw8. 3 Illapel, Chile earthquake, *Geophys. Res. Let.,* **43**(3), 961–966.

Okada, Y., 1985. Surface deformation due to shear and tensile faults in a half-space, *Bull. seism. Soc. Am.,* **75,** 1135–1154.

Pelinovsky, E.N. & Mazova, R.Kh., 1992. Exact analytical solutions of nonlinear problems of tsunami wave run-up on slopes with different profiles, *Nat. Hazards,* **6,** 227–249.

Pritchard, D. & Dickinson, L., 2007. The near-shore behaviour of shallow-water waves with localized initial conditions, *J. Fluid Mech.,* **591,** 413–436.

Riquelme, S., Fuentes, M., Hayes, G.P. & Campos, J., 2015. A rapid estimation of near field tsunami run-up, *J. geophys. Res.,* **120,** doi:10.1002/2015JB012218.

Sepúlveda, L., Liu, P. & Philip 2016. Estimating tsunami runup with fault plane parameters, *Coast. Eng.,***112,** 57–68.

Synolakis, C., 1987. Runup of solitary waves, *J. Fluid Mech.,* **185,** 523–545.

Synolakis, C., 1991. Tsunami runup on steep slopes: how good linear theory really is, *Nat. Hazards,* **4,** 221–234.

Synolakis, C., Liu, P., Philip, H.A., Carrier, G. & Yeh, H., 1997. Tsunamigenic sea-floor deformations, *Science,* **278**(5338), 598–600.

Synolakis, C., Bernard, E., Titov, V., Kânoğlu, U. & González, F., 2008. Validation and verification of tsunami numerical models, *Pure appl. Geophys.,* **165**(11–12), 2197–2228.

Tadepalli, S. & Synolakis C., 1994. The run-up of N-waves on sloping beaches, *Proc. R. Soc. A,* **445,** 99–112.

Tuck, E.O. & Hwang, L.-S., 1972. Long wave generation on a sloping beach, *J. Fluid Mech.,* **51,** 449–461.

APPENDIX A: DETAILED MATHEMATICAL DERIVATION

In the following, detailed derivations are shown step by step.

A1 The still water shoreline (SWS) motion $\eta(0, t)$

The linearized system (1)–(2) is the starting point. By elimination of $u(x, t)$, with $h(x) = \alpha x$, one obtains an equivalent second-order partial differential equation

$$\eta_{tt} - \alpha g(x\eta_x)_x = \eta_{0tt} \tag{A1}$$

Downloaded from https://academic.oup.com/gji/article-abstract/209/2/597/2957020
by Universidad de Chile user
on 22 March 2018

To solve eq. (A1), a Hankel-type transform is employed. The following definition will be adopted:

$$\mathcal{H}\{f\}(k) =: \hat{f}(k) =: \int_0^\infty f(r) J_0(2k\sqrt{r}) \mathrm{d}r \tag{A2}$$

$$f(r) = 2\int_0^\infty \hat{f}(k) J_0(2k\sqrt{r}) k \mathrm{d}k \tag{A3}$$

where J_0 is the cylindrical Bessel function of zero order. Note that the use of the elements $J_0(2k\sqrt{r})$ for the basis is guaranteed by the orthogonality of the Bessel functions. Also, a correct evaluation of the Dirac delta is needed. This comes from the fact that $\delta(g(x)) = \sum_i \frac{\delta(x-x_i)}{|g'(x_i)|}$, where the sum is over the roots of g.

The main reason of using eqs (A1) and (A2) is that the operator $(x\eta_x)_x$ is converted into $-k^2\hat{\eta}(k,t)$, in fact,

$$\begin{aligned}
&\mathcal{H}\{(x\eta_x)_x\}(k) \\
&= \int_0^\infty (x\eta_x)_x J_0(2k\sqrt{x}) \mathrm{d}x \\
&= \left[(x\eta_x) J_0(2k\sqrt{x})\right]_0^\infty + k\int_0^\infty \eta_x J_1(2k\sqrt{x})\sqrt{x}\mathrm{d}x \\
&= k\left[\eta J_1(2k\sqrt{x})\right]_0^\infty - k\int_0^\infty \eta(x,t)\left(J_1(2k\sqrt{x})\sqrt{x}\right)_x \mathrm{d}x \\
&= -k^2\hat{\eta}(k,t),
\end{aligned}$$

where the identity $(\frac{1}{x}\frac{\mathrm{d}}{\mathrm{d}x})^m (x^n J_n(x)) = x^{n-m} J_{n-m}(x)$ is used in the last step.

Then, eq. (A1) becomes

$$\hat{\eta}_{tt} + \alpha g k^2 \hat{\eta} = \hat{\eta}_{0tt}. \tag{A4}$$

Now, eq. (A4) can be solved by using the Laplace transform

$$\mathcal{L}\{f\}(s) = \overline{f}(s) =: \int_{0_-}^\infty f(t) e^{-st} \mathrm{d}t.$$

The lower limit 0_- makes emphasis on the fact that f can be also a distribution, for instance, the Dirac delta impulse. Thus, the Laplace transform turns the ODE (A4) into

$$s^2\overline{\hat{\eta}}(k,s) - s\hat{\eta}(k,0_-) - \hat{\eta}_t(k,0_-) + \alpha g k^2 \overline{\hat{\eta}} = \mathcal{L}\{\hat{\eta}_{0tt}\}(s). \tag{A5}$$

Solving for $\overline{\hat{\eta}}$,

$$\begin{aligned}
&\overline{\hat{\eta}}(k,s) \\
&= \frac{1}{s^2 + (\sqrt{\alpha g}k)^2}\left(\mathcal{L}\{\hat{\eta}_{0tt}\}(s)\right. \\
&\quad \left. + s^2\left[\frac{1}{s}\hat{\eta}(k,0_-) + \frac{1}{s^2}\hat{\eta}_t(k,0_-)\right]\right) \\
&= \frac{1}{s^2 + (\sqrt{\alpha g}k)^2}\left(\mathcal{L}\{\hat{\eta}_{0tt}\}(s)\right. \\
&\quad \left. + \mathcal{L}\{([\hat{\eta}(k,0_-) + t\hat{\eta}_t(k,0_-)]\,\mathcal{H}(t))_{tt}\}(s)\right) \\
&= \frac{1}{s^2 + (\sqrt{\alpha g}k)^2}\mathcal{L}\{(\hat{\eta}_0 + [\hat{\eta}(k,0_-) + t\hat{\eta}_t(k,0_-)]\,\mathcal{H}(t))_{tt}\}(s)
\end{aligned}$$

defining the function $\eta_1(x,t) =: \eta_0(x,t) + [\eta(x,0_-) + t\eta_t(x,0_-)]\,\mathcal{H}(t)$, where $\mathcal{H}(t)$ is the Heaviside step function, one has

$$\overline{\hat{\eta}}(k,s) = \frac{1}{s^2 + (\sqrt{\alpha g}k)^2}\overline{\hat{\eta}}_{1tt}(k,s). \tag{A6}$$

Utilizing the convolution theorem from eq. (A6) follows

$$\hat{\eta}(k,t) = \frac{\mathcal{H}(t)}{\sqrt{\alpha g}k}\sin\left(\sqrt{\alpha g}kt\right) * \hat{\eta}_{1tt}(k,t). \tag{A7}$$

Writing the convolution integral and replacing the Hankel transform definitions from eqs (A2) and (A3), eq. (A7) results in

$$\begin{aligned}
\eta(x,t) = \frac{2}{\sqrt{g\alpha}}&\int_0^\infty J_0\left(2k\sqrt{x}\right)\int_0^\infty J_0\left(2k\sqrt{\xi}\right) \\
&\times \int_0^t \eta_{1tt}(\xi,\tau)\sin[\sqrt{\alpha g}k(t-\tau)]\mathrm{d}\tau\,\mathrm{d}\xi\,\mathrm{d}k,
\end{aligned} \tag{A8}$$

which is the general solution for the water surface evolution.

As a particular case, $\eta_0(x,t) = \eta_t(x,0_-) = 0$ for all (x,t) are chosen. Thus, the definition of $\eta_1(x,t)$ implies

$$\eta_{1tt}(x,t) = \eta(x,0_-)\delta_t(t). \tag{A9}$$

This allows the integration on τ,

$$\begin{aligned}
&\int_0^t \eta_{1tt}(\xi,\tau)\sin[\sqrt{\alpha g}k(t-\tau)]\mathrm{d}\tau \\
&= \int_0^t \eta(\xi,0_-)\sin[\sqrt{\alpha g}k(t-\tau)]\delta_\tau(\tau)\mathrm{d}\tau \\
&= -\eta(\xi,0_-)\{\partial_\tau \sin[\sqrt{\alpha g}k(t-\tau)]\}\big|_{\tau=0} \\
&= \eta(\xi,0_-)\partial_t \sin[\sqrt{\alpha g}kt].
\end{aligned} \tag{A10}$$

Then, inserting eq. (A10) in eq. (A8) and utilizing the Leibniz integral rule give

$$\begin{aligned}
\eta(x,t) = \frac{2}{\sqrt{g\alpha}}&\int_0^\infty \eta(\xi,0_-)\partial_t \\
&\times \int_0^\infty J_0\left(2k\sqrt{x}\right) J_0\left(2k\sqrt{\xi}\right)\sin[\sqrt{\alpha g}kt]\mathrm{d}k\mathrm{d}\xi.
\end{aligned} \tag{A11}$$

Eq. (A11) suggests defining a function independent of the initial condition,

$$G(x,\xi,t) = \int_0^\infty J_0\left(2k\sqrt{x}\right) J_0\left(2k\sqrt{\xi}\right)\sin[\sqrt{\alpha g}kt]\mathrm{d}k. \tag{A12}$$

Eq. (A12) is interpreted as the Green's function of the system. Except that factors and definition of the variables, it is practically the same kernel obtained by Carrier *et al.* (2003). Therefore, in terms of G, the water surface evolution is written as

$$\eta(x,t) = \frac{2}{\sqrt{g\alpha}}\int_0^\infty \eta(\xi,0_-)G_t(x,\xi,t)\mathrm{d}\xi. \tag{A13}$$

To study the approximated shoreline motion, eq. (A13) is evaluated at $x = 0$. Employing the Leibniz's integral rule and (see e.g. Gradshteyn & Ryzhik 1994)

$$\int_0^\infty J_0(ax)\sin(bx)\mathrm{d}x = \frac{\mathcal{H}(b-a)}{\sqrt{b^2-a^2}} \tag{A14}$$

one can obtain

$$\eta(0,t) = \frac{2}{\sqrt{g\alpha}}\frac{\partial}{\partial t}\left\{\int_0^{\frac{1}{4}\alpha g t^2} \frac{\eta(\xi,0_-)}{\sqrt{\alpha g t^2 - 4\xi}}\mathrm{d}\xi\right\}. \tag{A15}$$

Last expression can be simplified by considering the change of variables inside the integral $\xi =: \frac{1}{4}\alpha g t^2 y$, which turns it into

$$\eta(0,t) = \frac{1}{2}\frac{\partial}{\partial t}\left\{t\int_0^1 \frac{\eta\left(\frac{1}{4}\alpha g t^2 y, 0_-\right)}{\sqrt{1-y}}\mathrm{d}y\right\}. \tag{A16}$$

Downloaded from https://academic.oup.com/gji/article-abstract/209/2/597/2957020
by Universidad de Chile user
on 22 March 2018

For numerical integration purposes, eliminating the singularity in the integrand is required. To complete this task, the change of variables $y = \sin^2(\theta)$ is employed, which turns (A16) into

$$\eta(0,t) = \frac{\partial}{\partial t}\left\{ t\int_0^{\frac{\pi}{2}} \eta\left(\frac{1}{4}\alpha g t^2 \sin^2(\theta), 0_-\right)\sin(\theta)\mathrm{d}\theta \right\}. \tag{A17}$$

At this point, eq. (A17) can be numerically used for integrating any analytical initial condition. Nonetheless, when the initial condition allows infinite derivatives around $x = 0$, eq. (A16) can be used to obtain a series expansion. There are, at least, two equivalent ways to obtain it: by iterative integration by parts and by McLaurin expansion of the initial condition. Only the second one is presented here. Therefore, writing

$$\eta(x^* y, 0_-) = \sum_{k=0}^{\infty} \frac{\partial_x^k \eta(0,0_-)}{k!}(x^* y)^k \tag{A18}$$

where $x^* = \frac{1}{4}\alpha g t^2$, expression (A18) is inserted into (A16) and integrating term by term follows

$$\eta(0,t) = \frac{1}{2}\sum_{k=0}^{\infty} \frac{\partial_x^k \eta(0,0_-)}{k!}\partial_t\left(t x^{*k}\right)\int_0^1 y^k (1-y)^{-\frac{1}{2}}\mathrm{d}y. \tag{A19}$$

The integral on eq. (A19) is the Beta function which can be evaluated in exact form (see e.g. Abramowitz & Stegun 1964)

$$\int_0^1 y^k (1-y)^{-\frac{1}{2}}\mathrm{d}y = \mathrm{B}\left(k+1,\frac{1}{2}\right) = \frac{2^{k+1}k!}{(2k+1)!!} \tag{A20}$$

where $(2m+1)!! =: \prod_{i=0}^{m}(2i+1)$, with $(-1)!! =: 1$.

Finally, inserting eq. (A20) into (A19) and using $\partial_t(t x^{*k}) = (2k+1)x^{*k}$

$$\eta(0,t) = \sum_{k=0}^{\infty} \frac{(2x^*)^k}{(2k-1)!!}\partial_x^k \eta(0,0_-), \tag{A21}$$

which is the series representation of the approximated shoreline motion when the initial condition admits McLaurin expansion around $x = 0$.

A2 The approximated shoreline velocity $u(0, t)$

Taking eq. (A12) and using that $\lim_{z\to 0}\frac{J_1(z)}{z} = \frac{1}{2}$,

$$\begin{aligned} G_x(0,\xi,t) &= \partial_x \int_0^{\infty} J_0\left(2k\sqrt{x}\right) J_0\left(2k\sqrt{\xi}\right)\sin[\sqrt{\alpha g}kt]\mathrm{d}k\Big|_{x=0} \\ &= -\int_0^{\infty} k\frac{J_1\left(2k\sqrt{x}\right)}{\sqrt{x}} J_0\left(2k\sqrt{\xi}\right)\sin[\sqrt{\alpha g}kt]\mathrm{d}k\Big|_{x=0} \\ &= -\int_0^{\infty} k^2 J_0\left(2k\sqrt{\xi}\right)\sin[\sqrt{\alpha g}kt]\mathrm{d}k \\ &= \frac{1}{\alpha g}G_{tt}(0,\xi,t). \end{aligned} \tag{A22}$$

Inserting eq. (A22) into eq. (A13), the spatial derivative is

$$\begin{aligned} \eta_x(0,t) &= \frac{1}{\alpha g}\frac{2}{\sqrt{\alpha g}}\int_0^{\infty}\eta(\xi,0)G_{ttt}(0,\xi,t)\mathrm{d}\xi \\ &= \frac{1}{\alpha g}\eta_{tt}(0,t). \end{aligned} \tag{A23}$$

Then, from eq. (1) and replacing eq. (A23),

$$u_t(0,t) = -\frac{1}{\alpha}\eta_{tt}(0,t). \tag{A24}$$

Because of the null initial velocity condition, integration of eq. (A24) gives

$$u(0,t) = -\frac{1}{\alpha}\eta_t(0,t), \tag{A25}$$

which is the formula used to estimate the linear approximation of the shoreline velocity.

Downloaded from https://academic.oup.com/gji/article-abstract/209/2/597/2957020
by Universidad de Chile user
on 22 March 2018